Application of perforated PEEK framework for improving strength of a bases of removable complete denture for maxilla

Kamalutdin Akhmedov, Dmitry Arutyunov, Mikhail Lomakin
Russian University of Medicine, 127006, Moscow, Russia
kama05doc@gmail.com, http://orcid.org/0009-0000-5195-3942
dmitry.arutyunov@icloud.com, http://orcid.org/0009-0002-9325-2751
lomakin_mv@mail.ru, http://orcid.org/0000-0003-3739-6275

Svetlana Bochkareva, Iliya Panov, Sergey Panin
Institute of Strength Physics and Materials Science of the Siberian Branch of the Russian Academy of Sciences (ISPMS SB RAS), 634055, Tomsk, Russia,
svetlanab7@yandex.ru, http://orcid.org/0000-0003-4889-6128
panov.iliya@mail.ru, http://orcid.org/0000-0003-2321-7109
svp@ispms.ru, http://orcid.org/0000-0001-7623-7360

Magomet Mustafaev, Sofiat Mustafaeva
Kabardino-Balkarian State University, 360004, Nalchik, Russia
musmag@mail.ru, http://orcid.org/0000-0002-4042-9421
666238@mail.ru, http://orcid.org/0000-0003-2645-4089

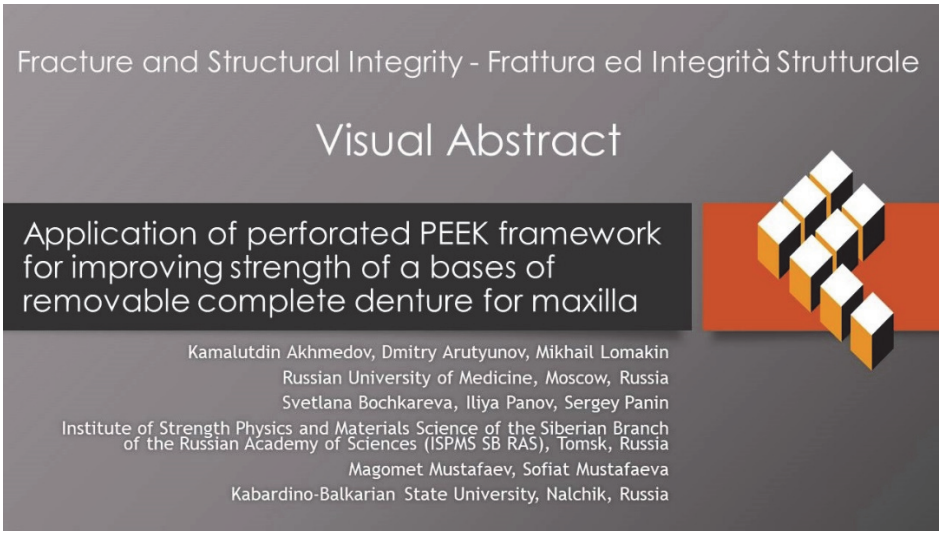

KEYWORDS. Computer aided engineering (CAE), Structural integrity, Failure, removable complete denture (RCD), Polymethylmethacrylate (PMMA), Polyetheretherketone (PEEK), Additive manufacturing, Prosthesis framework, Finite Element Method (FEM), Failure criterion, Interlayer adhesion.

OPEN ACCESS

Citation: Akhmedov K, Arutyunov D., Lomakin M., Bochkareva S., Panov I., Panin S., Mustafaev M., Mustafaeva S. Improving mechanical properties of complete removable dentures for the maxilla by reinforcing their bases with perforated peek frameworks, Fracture and Structural Integrity, 72 (2025) 280-294.

Received: 07.02.2025
Accepted: 21.03.2025
Published: 26.03.2025
Issue: 04.2025

INTRODUCTION

The population aging is one of the inevitable consequences of the gradual improvement in the life quality [1, 2]. This results in a fact that people may (partially) lose a number of vital functions, including tooth loss due to various reasons [3–5]. In some cases, this problem is solved by application of removable complete dentures (RCDs), the warranty period of which is varied from one to five years, depending on the country [5–6]. First of all, it is limited by worn out of cosmetic teeth in dentitions and failure of the RCD bases [7–10]. To reduce the production cost, dental polymers are used, primarily polymethyl methacrylate (PMMA) [11, 12].

Dental products and structures made of PMMA can also be fabricated by additive manufacturing [13–15], which significantly reduces both time and costs, as well as enables to implement up-to-date digital technologies for reproduction of the anatomical features of each specific patient upon making RCDs. Despite all the advantages of using this polymer (the possibility of manufacturing and subsequent individualization by a dental technician), its mechanical properties are far from the highest levels [16, 17]. Due to this reason, some researchers have suggested to embed reinforcing meshes, made of various metals (i.e. steels), glasses, nylon and polyethylene fibers [18–22] (or even frameworks [23]), especially with regard to the RCDs of the maxilla that include the palatal domes. However, the aspects of both adhesion and manufacturability when embedding them into the polymer (PMMA) bases are the key limiting factors [24], in spite of the high mechanical properties of the reinforcing metal meshes. In addition, they increase both weight and mechanical incompatibility (difference in elastic moduli) of the components of such layered structures [25].

When discussing the aspects of reinforcing RCDs from the standpoint of the structural mechanics, it is important to note the main reasons of their failure:

1. The area and the pattern of supports of the RCDs on alveolar ridge are not constant, during both a single day (short-term conditions upon wearing or mastication) and the entire operational period (long-term conditions associated with a gradual decrease in heights of the alveolar ridge, for example, due to bone resorption) [26, 27]. In this regard, the RCDs as a component of the 'prosthesis–mucous membrane–alveolar ridge' biological structures can be exposed to non-axial loads that significantly exceed the average statistical levels of 100 N upon mastication [28].
2. V-shaped notches are cut in the central parts of the RCD bases to isolate frenulums [29]. Being a stress raiser, the notches can cause the initiation of cracks at the notch tips and their propagation resulting in failure of the bases.
3. During mastication, the anterior teeth may experience differently oriented loads, which may cause the development of overturning stresses [30]. As a result, the RCDs change their support conditions and experience local overloads, contributing to their premature failure.
4. Dentitions are characterized by inconsistent cross sections and their fixation is carried out by packing PMMA doughs, so stress raisers can also be found at the fixation points.

It is known [31] that reinforcing meshes and frameworks made of high-strength polymers can be an alternative to the use of metal ones. So, the operational performance of RCDs can be improved by integrating of reinforcing frameworks from more durable polymers into the PMMA base domes. To prove this hypothesis, computer simulation of the operation of such structures should be performed. Its results enable to evaluate possible changes in the stiffness/strength/load-bearing capacity of the RCDs with such reinforcements by varying their parameters before solving the technological issues of their manufacture and integration into the base domes.

In this study, the problem of embedding of perforated reinforcing frameworks from polyetheretherketone (PEEK) into the PMMA bases of RCDs was considered. PEEK possesses higher strength properties compared to those of PMMA and can be used as a feedstock in additive manufacturing. By computer simulation, changes in the stress–strain states (SSSs) of the RCDs were analyzed [32]. In these cases, variations of the support conditions (due to the degradation of the alveolar ridge caused by bone resorption) were considered as one of the key causes of failure. The null hypothesis was the possibility of improving both stiffness and strength of the RCDs by embedding the PEEK frameworks.

STATEMENT OF THE PROBLEM

The authors of this paper have developed an individual digital model for a RCD of the maxilla made of PMMA, fabricated according to the analogue protocol [29] with an additively-manufactured perforated PEEK framework in its base [33]; the model was exported into 'ABAQUS' code then (Fig. 1). Cosmetic teeth, which comprised an individual dentition, were attached to the base. As noted above, a V-notch is made in the front part of the base for the frenulum (shown by a circle in Fig. 1, a), as well as ones of individual shapes according to anatomical features (cords on

both sides, marked by an oval in Fig. 1, b). The cosmetic teeth had a visible part protruding above the base and a hidden layer recessed into it (in sockets according to Fig. 1, b). The contact area between the cosmetic teeth and the base is clearly visible in Fig. 1, b, where the only PMMA base is shown. In real RCDs, dental arches and bases are joined with PMMA-based adhesives, so the conditions for the dentition attachment to the base were taken into account.

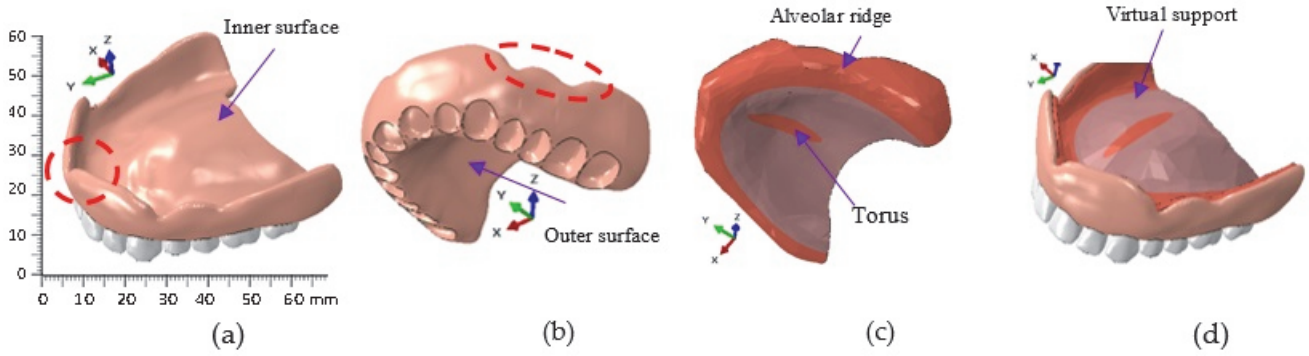

Figure 1: The model of the RCD of the maxilla with the cosmetic teeth (a) and without it (b); the virtual support, indicating the areas of both alveolar ridge and torus (c); the model of the RCD with the virtual support (d); ideal adhesion.

In order to justify boundary conditions close to the real ones for supporting and fixing RCDs, a virtual support was added to the model, reflecting the typical shape of an alveolar ridge of the maxilla (Fig. 1, c and d). Thus, the RCD based on the virtual support instead of the alveolar ridge in computer simulation.

The load-bearing capacity of the RCD, both with the PEEK framework and without it, was assessed by analyzing its SSSs under operational loads by applying the finite element method (FEM). The problem was solved using the 'ABAQUS' FEM-based software package, v. 2019 (Dassault Systemes, France) in the linear-elastic static formulation implemented in the 'ABAQUS/Standard' module.

The boundary conditions from the inner side of the virtual support assumed its immobility; in doing so the displacements along all the axis as well as any rotations were zeroed (Fig. 1, d). In the contact between the RCD and the virtual support, the ideal adhesion conditions were preset, reflecting the suction of the prosthesis to the maxilla. This statement corresponded to the conditions of both normal and tangential contacts without friction for the 'ABAQUS' software package (Normal behavior – 'Hard contact' and Tangential behavior – 'Frictionless'), which prevents mutual penetration of adjacent materials. The contact stiffness ('Cohesive behavior') of 30 MPa was assumed to be the same in all regions. For providing the contact restrictions, the direct method was used by default, which ensured strict observance of the 'rigid' connection between the contacting surfaces due to the equality of forces and moments. As a result, the mating surfaces could not penetrate into each other.

In the virtual support (Fig. 1, c), areas with different mucosal compliance were identified (according to E.I. Gavrilov [34]): the alveolar ridge area (along the perimeter of the RCD) and the torus (in the center), which were characterized by negligible mucosal compliance, i.e. lower damping properties than those at other regions [35]. Due to this reason, the elastic modulus of both alveolar ridge and torus was taken to be 30 MPa, while it was 5 MPa in all other regions of the virtual support [36], simulating different compliance of the mucous membrane of the palate. Poisson's ratio was assumed to be 0.45.

The materials were assumed to be elastic and isotropic. The elastic modulus of the cosmetic teeth was assumed to be 2.2 GPa under both tensile and compressive loads (corresponding to ones fabricated by additive manufacturing from the PMMA/GF composite). For the base, the mechanical properties corresponded to those of the 'NOLATEK 3D LCD/DLP' PMMA feedstocks ('VladMiVa' LLC, Belgorod, Russia), namely the tensile elastic modulus of 0.9 GPa and the ultimate tensile strength of 22 MPa [30]. Its Poisson's ratio was assumed to be 0.3. In computer simulation, the values determined in tensile tests were applied, since they were typically several times lower than those for both compression and shear ones [37]. Accordingly, such a scheme made it possible to ensure a certain margin of safety. Regardless ethe assumed elastic response of the materials under study, the calculations took geometrical nonlinearity into account. In addition, step-by-step loading was implemented. Since the stiffness of the virtual base was low, large strains could develop. Thus, rebuilding of the stiffness matrix would be necessary at every computational step.

The initiation and propagation of cracks were simulated using the extended FEM (XFEM) algorithms.

When developing the FEM model, C3D8R volumetric tetrahedral elements with linear approximation of displacements were used. Based on the data on mesh convergence, the following optimal number of FE-elements and nodes were

established: 959486 elements and 206441 nodes, excluding the PEEK framework, which additionally consisted of 1176187 elements and 421657 nodes.

CALCULATION OF SSSs OF THE RCD WITHOUT A FRAMEWORK

Over time, the alveolar ridge height could decrease locally (due to bone resorption), changing its shape and volume. To assess the effect of this process on the load-bearing capacity of the RCD, its SSSs were calculated considering such patterns by partially reducing the virtual support height. This phenomenon was simulated by deforming the virtual support in the anterior part of the base (shown by a red oval in Fig. 2, b). As a result, the virtual support locally did not fit tightly to the base; in doing so, the contact was absent in the region.

Figure 2: The RCD with the initial (a) and deformed (b) virtual supports

The SSSs were calculated for different loading conditions, which corresponded to the impact of **symmetrical** and **asymmetrical** operational loads upon biting or chewing food. Under the **symmetrical** loads, the following options were considered:

1) No.1 on four incisors at an angle of 30 ° (Fig. 3, a),
2) No.2 on four incisors at an angle of 0 ° (hereinafter, relative to the vertical axis of the teeth, according to Fig. 3, b),
3) No.3 on both two canines and two premolars at the angle of 0 °,
4) No.4 on both two canines and four incisors at the angle of 0 °;

while they were the following under the **asymmetrical** loads:

5) No.5 on both two premolars and two molars at the angle of 0 °,
6) No.6 on both one incisor and one premolar at the angle of 0 °,
7) No.7 on both one canine and one incisor at the angle of 0 °,
8) No.8 on two incisors, one canine and one premolar at the angle of 0 ° (Fig. 3, c),
9) No.9 on both three incisors and one canine at the angle of 0 °,
10) No.10 on two premolars at the angle of 0 °.

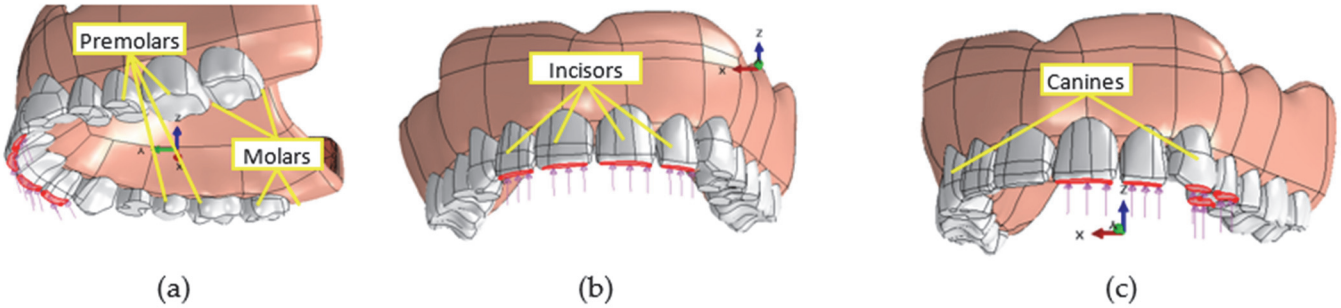

Figure 3: The loading options for the RCD: (a) No.1 – on four incisors at the angle of 30°, (b) No.2 – on four incisors at the angle of 0°, and (c) No.8 – on two incisors, one canines and one premolar at the angle of 0°

The loads were simultaneously applied to several teeth. At the same time, they were distributed equally to each of the teeth. As a criterion for assessing the loss of the load-bearing capacity, which corresponded to the initiation of a crack upon reaching the threshold for the PMMA base, the maximum (tensile) principal stresses of 22 MPa were taken; this made it possible to consider the fracture processes induced due to the development of tensile stresses (since the tensile strength of the PMMA is multiply less in contrast the compression strength) [30].

Results of calculations of SSSs of the RCD with the initial and deformed virtual supports

Fig. 4 shows diagrams on calculated ultimate loads (on each of the loaded teeth), i.e. their load-bearing capacities, corresponding to the crack initiation (according to the accpeted failure criterion). In the case of the deformed virtual support, the mechanical properties of the base were mainly reduced, although they remained almost constant under some loading conditions. The reason was the deformation of the virtual support, since its contact with the base was set as ideal. Respectively, the base was reliably fixed on some parts of the virtual support even with partial local absences of contact zones. So, this presetting allowed the base to withstand loads similar to those for the nondeformed virtual support.

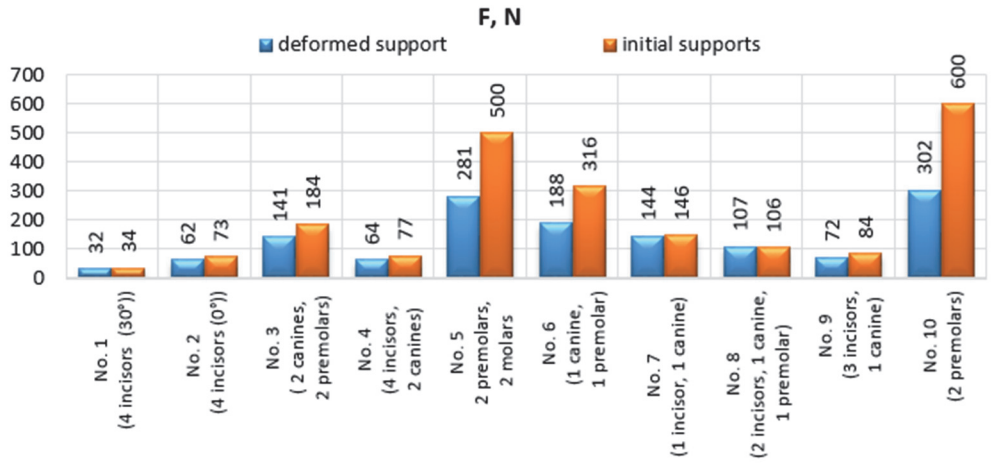

Figure 4: The ultimate loads (per tooth) for the RCD with the initial and deformed virtual supports under various loading conditions

By comparing the obtained results, it could be concluded that the most critical was option No.1 under the symmetrical loading conditions (the ultimate load per tooth of 32 N was minimal, while its total value for all loaded teeth was 128 N). Under the asymmetrical loading conditions, their minimum levels were revealed for option No.9 (72 and 288 N, respectively).

Upon loading, the teeth could be turned (possibly in different directions), causing the action of turning moments on the base that bent it. Even if the loading direction coincided with the vertical axis of the tooth (for example, on the incisors at the angle of 0 °, according to Fig. 5, a), the rotation of the teeth took place (since it was not parallel to the normal to the plane of their support). So, the teeth bent the base due to the action of tangential stresses, as it was reported in [14]. Typical patterns of base bends are shown in Fig. 5 in terms of principal stresses (including at a 40-fold zoom in the strain scale) under different loading conditions. Here and below, the values of stresses are given in MPa, displacements are presented in millimeters, while strains are dimensionless.

The most obvious options No.2, No.3 and No.6, shown in Fig. 5, reflected the deformation of the base due to the bending. The locations of cracks in the base are indicated by arrows: the red ones are oriented normal to the directions of their propagation, while the blue lines are parallel. In most cases, the cracks initiated between the teeth due to the tensile stresses in the base, which mainly arose because of the rotation of the teeth in different directions (Fig. 5, a and b). Two exceptions were options No.5 and No.6 with the deformed virtual support, when cracks initiated in the notches for the cords (Fig. 5, c). The main cause was the overbending of the base in the alveolar ridge, when tensile stresses developed in the notches for the cords due to the compressive loads on the teeth. With asymmetric loading on both premolars and molars (option No.5), the turning moment along the tooth axis either was not observed or was characterized by a small value (in contrast to the other options). For this reason, the applied compressive load was concentrated at the area of the base under these teeth (the alveolar ridge), as a result of which the base was bent precisely in this region.

According to Fig. 5, b and c, great compressive stresses extended from the premolar to the outer surface of the base. At the same time, the area located under the bending point (on the edge of the base) experienced tensile stresses. Since the ultimate

compressive stresses were twice as large as the tensile ones, a crack initiated in the tensile area, just in the notches for the cords (Fig. 5, c).

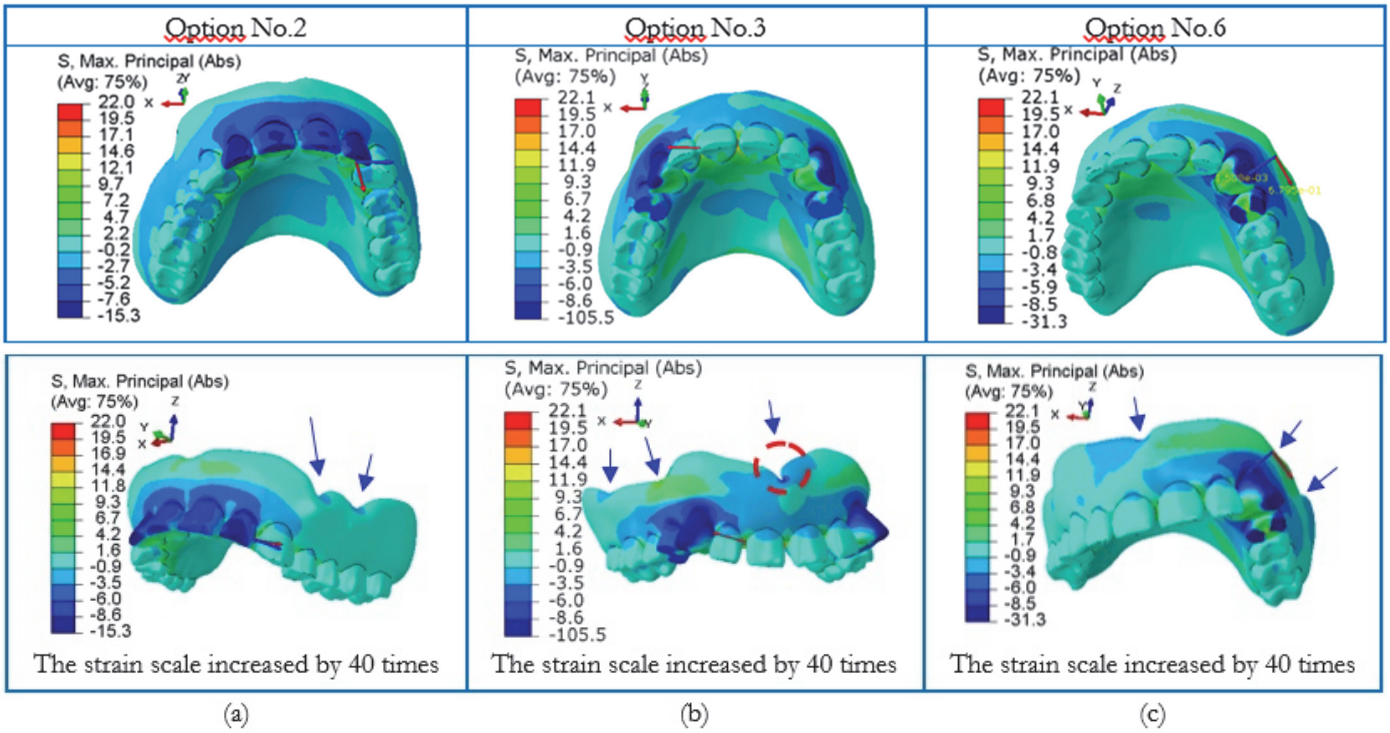

Figure 5: Distributions of the maximum principal stresses (MPa) in the RCD (without scaling (top) and with the 40-fold zoom in the strain scale (bottom)) for different loading conditions: (a) option No.2; (b) option No.3; (c) option No.6; the incomplete 'base–virtual support' contacts

In all cases, the edge of the base was bent in the regions of the notches for both frenulum and cords (indicated by arrows in Fig. 5), where tensile and compressive stresses were localized. In adjacent areas, stresses were characterized by the opposite sign, as a rule. If tensile stresses developed in the notches for the cords, then they were compressive in the notch for the frenulum, and vice versa. Therefore, in addition to static cracks in the notches of the base, fatigue damage could accumulate over time.

For the option No.4, comparison of the calculated SSSs showed that bending of the base was smaller (at high loads) for the RCD with the initial virtual support than that for the deformed one (Fig. 6, highlighted by an oval). Upon loading, the teeth rotated in different directions for both virtual supports, contributing to turning moments in the base and its bending. For this reason, the maximum tensile stresses were in the base at the areas between the tooth sockets, leading to the initiation of cracks. With the deformed virtual support, a crack initiated in the base between the canine and premolar (Fig. 6, b) due to the greater bending of the base in this region. This phenomenon was different from that for the initial virtual support, when a crack initiated between the incisor and canine (Fig. 6, a).

Due to the action of the turning moments in the loaded teeth, both negative (compressive) and positive (tensile) stresses were observed on the palatal surface of the base (i.e. behind the dental arch, where tensile ones arose, according to Fig. 6) and on the vestibular surface (i.e. in front of the teeth, where compressive stresses developed). With the deformed virtual support (Fig. 6, b), compressive stresses increased in the area of the torus in the base due to the support features, providing a different pattern of the stress distribution. For this reason, a crack initiated at a different area in this case.

Different stress distributions in the virtual supports reflected variations in the support conditions for the base (Fig. 6). In the RCD with the deformed virtual support (Fig. 6, b), stresses were almost zero, since there were no contacts with the base. In other areas, stresses were greater and had a negative sign compared to those for the RCD with the nondeformed support (Fig. 6, a). Taking into account the deformation of the virtual support, the maximum displacements in the base increased from 0.130 mm (for its initial state) up to 0.273 mm (with the deformed one) at the maximum loads of 77 and 64 N, respectively (Fig. 4).

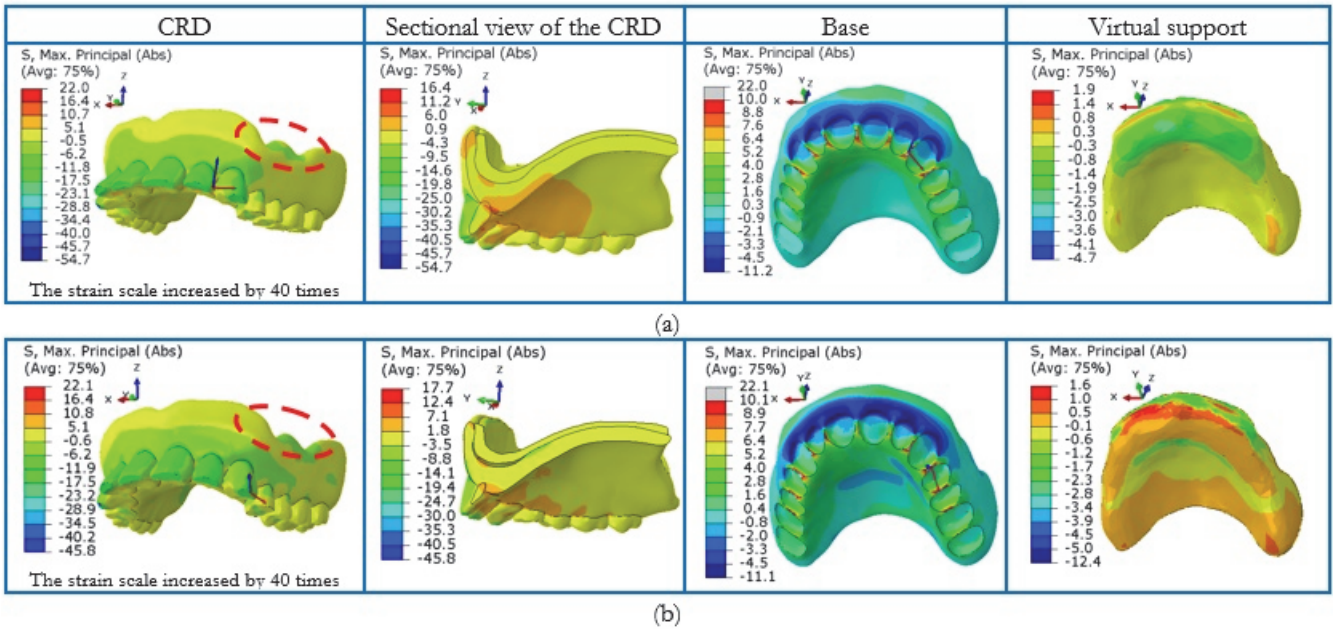

Figure 6: Distributions of the maximum principal stresses (MPa) in the RCD (option No.4), the base, as well as the initial (a) and deformed (b) virtual supports.

Thus, the load-bearing capacity of the base decreased with alveolar bone resorption due to the low ultimate tensile strength of PMMA (22 MPa). In some cases, this polymer did not withstand the minimum operational load per tooth of about 50 N [38]. As noted above, it was possible to improve the load-bearing capacity of RCDs by the embedding the reinforcing perforated frameworks inside the palatal dome of the base.

CALCULATION OF SSSS OF THE RCD WITH THE PEEK FRAMEWORK

In dental practice, reinforcing meshes (metal or polymer) are used to increase both stiffness and strength of RCDs of the maxilla. The most common are metal ones [24, 25], but the development of additive manufacturing and the invention of new high-strength polymers made it possible to use reinforcing frameworks from them. As mentioned above, the authors did not consider the aspects of production routes for the manufacturing such structures, since the key task was to evaluate the prospects of the solution from the mechanics standpoint.

A model of the PEEK framework with perforated holes 2 mm in diameter repeated the shape of the inner surface of the base (Fig. 7, a and b). The perforation was intended to increase its adhesion to the base by flowing PMMA through the holes (Fig. 7, c). As an idealization, the ideal adhesion conditions were preset between the PEEK framework and the base, while the following mechanical properties were applied for PEEK [39]: the elastic modulus of 3600 MPa and the ultimate tensile strength of 92 MPa. Similar to the results described above, alveolar bone resorption was considered via the deformation of the virtual support (Fig. 2).

As shown above, the base was deformed to a greater extent in the alveolar ridge area under loading, so changing the PEEK framework location in this region had to affect the mechanical properties of the base. To assess the effect of this factor on the load-bearing capacity of the RCD, the PEEK framework was located at the following areas (Fig. 8):

1) on the inner side of the base, i.e. in the contact with both palate and alveolar ridge (Fig. 8, a);
2) in the center of the base dome relative to its thickness (Fig. 8, b);
3) as close as possible to the outer side of the base (Fig. 8, c).

In addition, a solid PEEK framework (without holes) was considered to evaluate the effect of perforation, located in the center of the base (Fig. 8, d) by analogy with the one presented in Fig. 8, b. As in the previous cases, both initial and deformed virtual supports were considered. Since the minimum thickness of the base in the dome area was about 2.0–3.0 mm and it was 1.0–1.5 mm for the PEEK framework, its displacement from the inner surface of the base (from the side of both palate and alveolar ridge) to the center was ~0.5 mm (Fig. 8, b) and the displacement closer to the outer side was ~0.7 mm (Fig. 8, c).

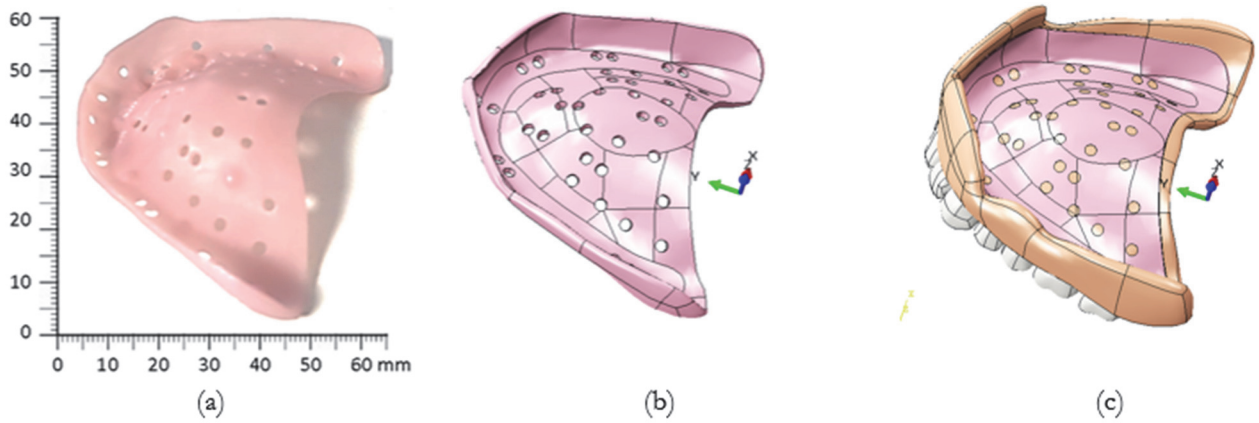

Figure 7: An additively manufactured polymer prototype for the model of the PEEK framework (a), the model separately (b) and inserted inside of the base (c).

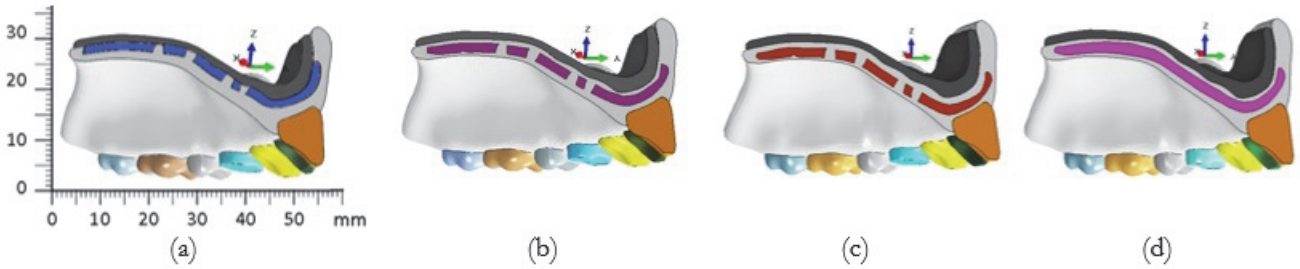

Figure 8: The RCD with the PEEK framework located: (a) on the inside, (b) in the center, and (c) on the outside; (d) represents the case but without perforated holes in the framework.

Comparison of SSSs of the RCD with different locations of the PEEK framework

Among the loading options considered above, those characterized by the minimal mechanical properties were applied, namely No. 1–4 and No. 7–9. According to the calculated data, the use of the perforated PEEK framework increased the load-bearing capacity by ~20–40% for the RCD with both initial (Fig. 9, a) and deformed (Fig. 9, b) virtual supports. At the same time, different locations of the PEEK framework enhanced this parameter by ≤10%.

In all studied cases, the load-bearing capacities of the RCD were predominantly lower when the perforated PEEK framework was located closer to the outer side of the base (Fig. 9). When it was located in the center or on the inner side of the base, these values were almost the same, differing within the calculation error of 5%. The absence of the perforation increased the load-bearing capacity of the base within similar ranges (probably for the same reason), with the exception of options No. 2 and No. 9.

It should be noted that the load-bearing capacities of the base with both the PEEK framework and the deformed virtual support turned out to be greater than that for the initial one in a number of cases. For option No. 8, the RCD with the deformed virtual support withstood slightly higher loads of 124–132 N (Fig. 9, b) than those of 118–124 N for the initial one (Fig. 9, a). However, the opposite was true without a framework (Fig. 4). The difference was within 10%, so the reason could be a combination of the applied load, the presence of the PEEK framework and the deformation of the virtual support. As a result, stresses were redistributed, increasing in the load-bearing capacity of the base.

Fig. 10 shows a comparison of the SSSs of the RCD with the deformed virtual support for option No. 9 with the PEEK framework located in the center of the base dome and closer to the outer surface. In both cases, the load-bearing capacities of the RCD and its SSSs were similar, but the areas of the initiation of cracks were different (these patterns were also typical for other loading options, so the authors did not consider them separately in detail). Since the virtual support was deformed in these cases, the maximum compressive stresses were distributed equally both in the denture base and in the PEEK framework, i.e. they were concentrated in front of the RCD (in the vestibular region) and in the torus area. In the PEEK framework, compressive stresses of ~13.9 MPa were slightly higher when it was located closer to the outer surface of the base than that of ~11.1 MPa, when it was in the center. At the same load of 88 N per tooth, displacements were smaller both in the base (0.249 mm) and in the PEEK framework (0.214 mm) when the latter was located in the center than those for the outer side of the base dome (0.288 and 0.256 mm, respectively). Thereby, the location of the PEEK framework in

the center of the base dome provided the greater load-bearing capacity with the deformed virtual support than that, when it was closer to the outer surface of the base.

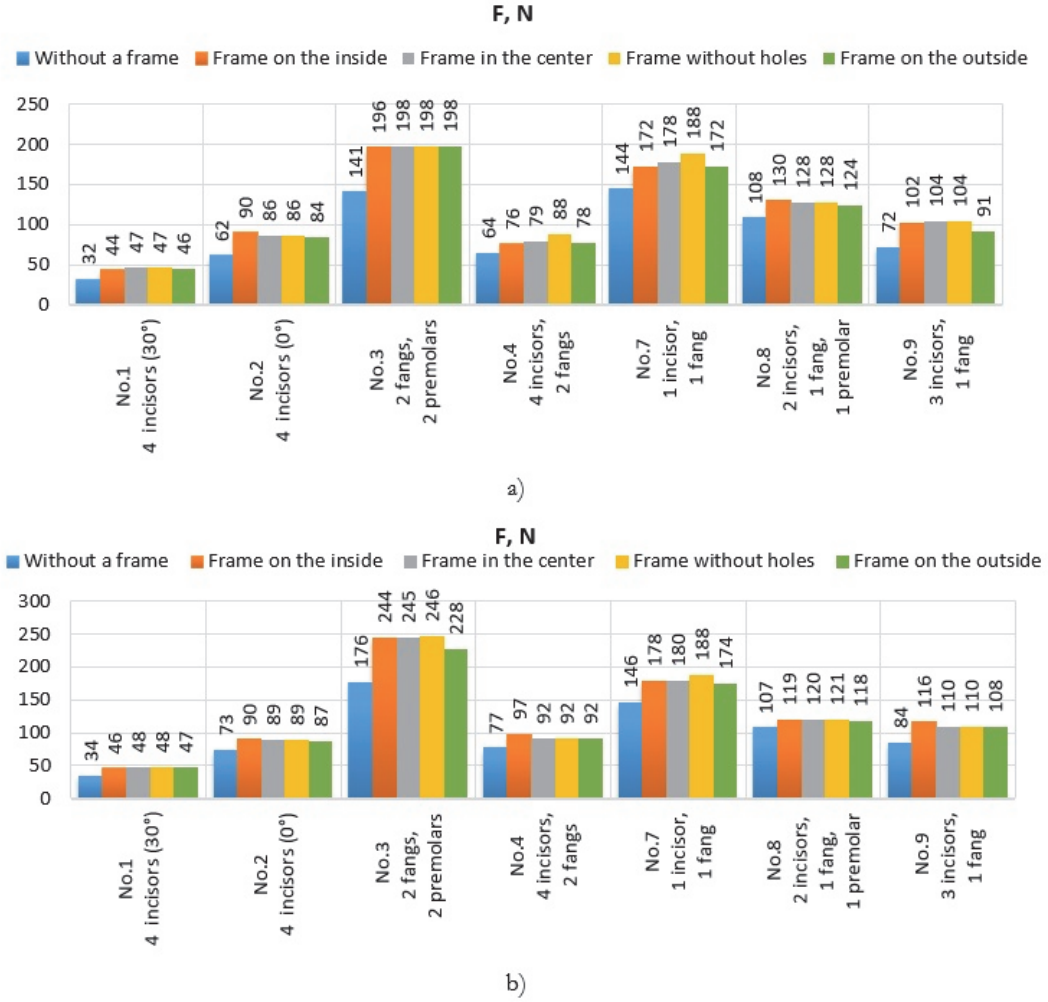

Figure 9: The ultimate loads for the RCD with different locations of the perforated PEEK framework (and without it) under various loading conditions; the initial (a) and deformed (b) virtual supports.

For option No. 4, the presence of the PEEK framework in the center (Fig. 11) reduced bending of the based compared to that without a framework (Fig. 5, c) with both initial and deformed supports. Upon loading, the base slightly changed its shape since compressive stresses were lower at the contact with the virtual support. For this reason, less bending was observed in the area of the notch for the frenulum under a greater load (highlighted by a circle in Fig. 11, b). Localization of tensile stresses between the sockets of the cosmetic teeth (Fig. 11) was caused by their rotation due to both applied load and bending of the base (as in the case of the RCD without a framework under the same conditions, according to Fig. 5, b). For both virtual supports, cracks initiated along the axis of symmetry of the base in the presence of the PEEK framework (Fig. 11), in contrast to that without a framework (Fig. 5, b). The reason was the fact that the PEEK framework, in addition to the reinforcement function, redistributed the load more uniformly with both initial and deformed virtual supports.
For both virtual supports, compressive and tensile stresses were concentrated on the inner area of the base (from the alveolar ridge side) in the region of the notch for the frenulum and cords, similar to the above considered cases. For the deformed virtual support (Fig. 11, b), compressive stresses increased at the area of the torus in the base, as for the PEEK framework. This fact was caused by a decrease in the support area of the base in the alveolar ridge region. In the PEEK framework, the maximum compressive stresses were above 14.2 MPa (at the low load) than that of 10.8 MPa for the initial virtual support (Fig. 11, a). In the virtual supports, they lowered from 14.2 down to 6.5 MPa due to the deformation and the reduction of the contact area with the base. In the base and the PEEK framework, displacements were smaller by approximately 1.5–1.7 times for the initial virtual support (Fig. 12).

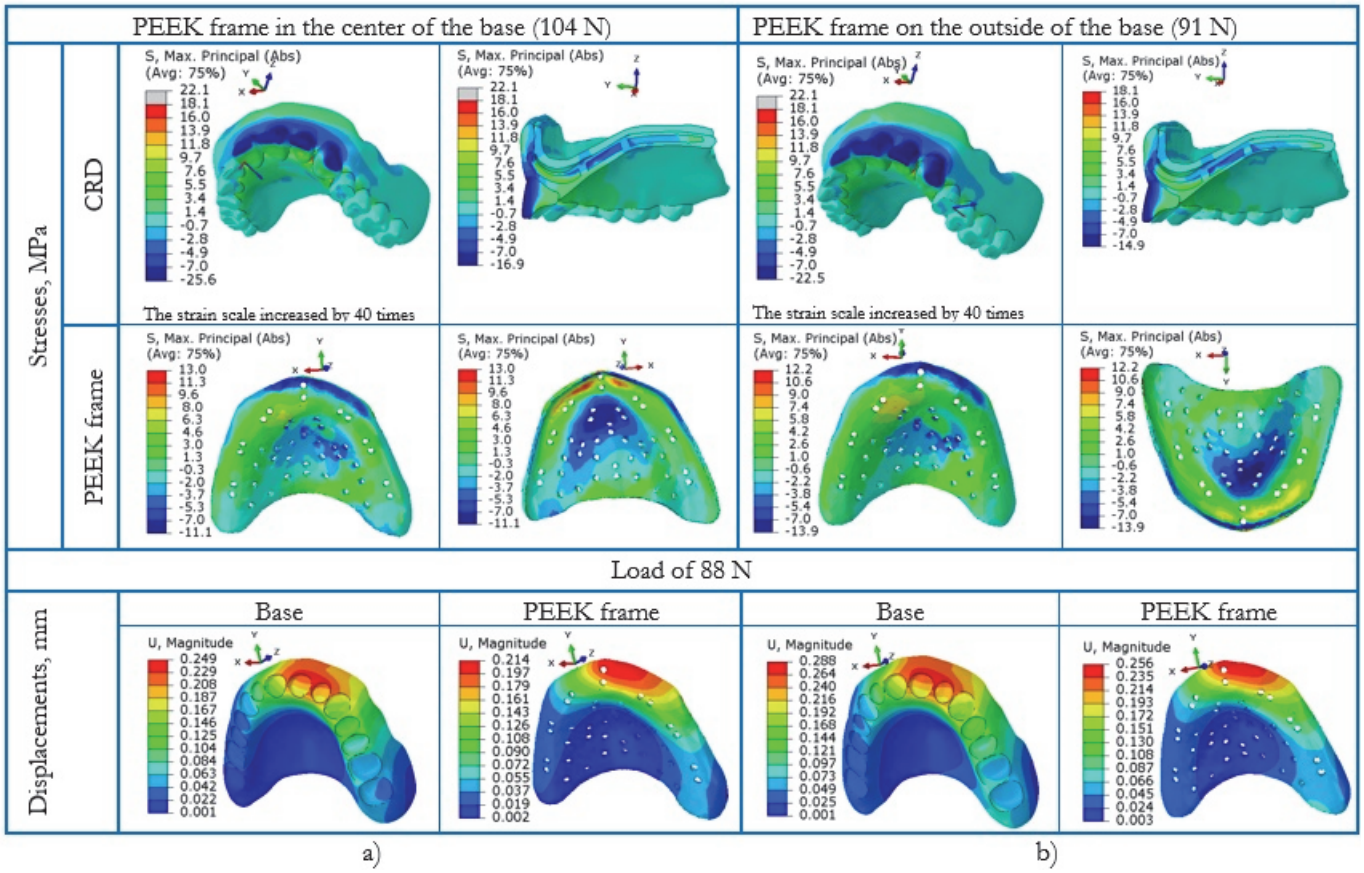

Figure 10: Distributions of the maximum principal stresses and displacements in the RCD, the base and the PEEK framework for its locations in the center (a) and on the outside of the base (b); option No. 9, the deformed virtual support.

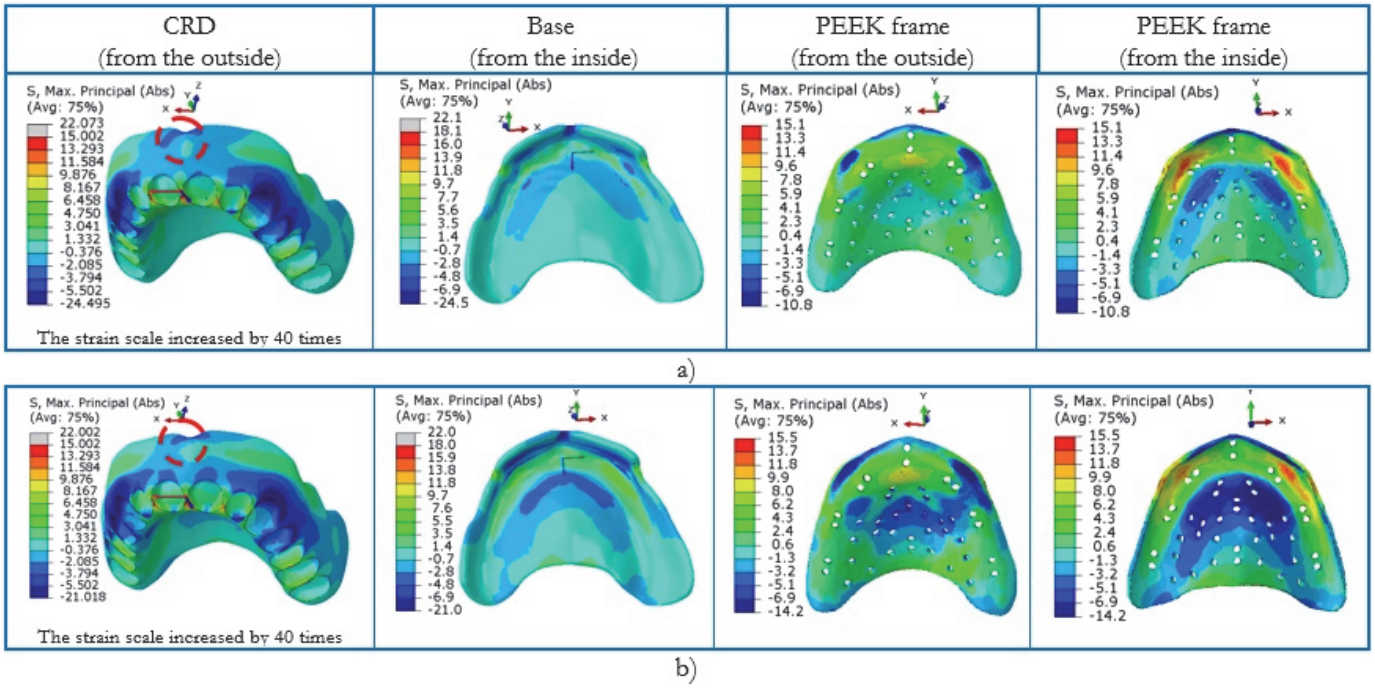

Figure 11: Distributions of the maximum principal stresses (MPa) in the base and PEEK framework for the RCD with the initial (a) and deformed (b) virtual supports

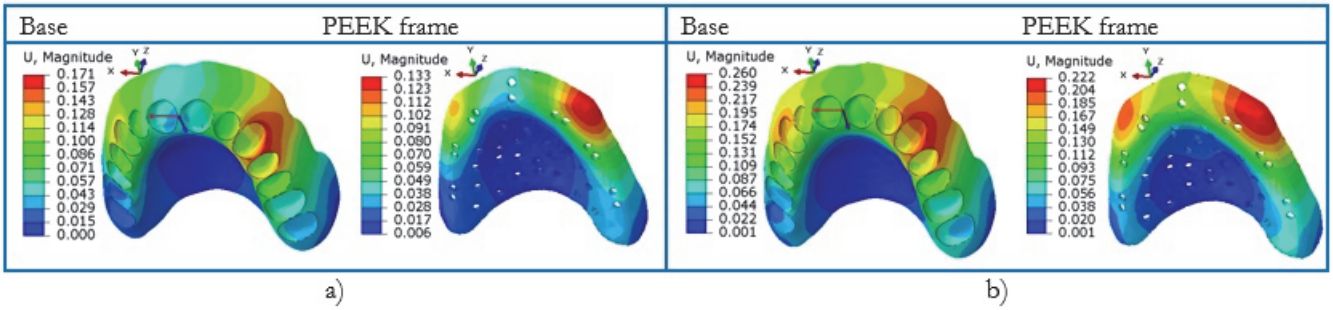

Figure 12: Distributions of displacements (mm) the base and the PEEK framework for the RCD with the initial (a) and deformed (b) virtual supports.

Thus, the greatest load-bearing capacity of the base was ensured by the location of the PEEK framework in its center and on the inner surface of the dome (in the contact with the alveolar ridge), while the lowest levels were observed for its location closer to its outer side. Changing the location of the PEEK framework varied the load-bearing capacity of the RCD by ≤10%. Such a phenomenon was expected, since it was increased primarily due to lower bending of the base. For this reason, frameworks should be more stiff, for example, via increasing their thicknesses or using stiffeners, instead of slightly changing their positions. However, such innovations are less convenient for patients.

The obtained results showed that the embedding of the PEEK framework allowed to withstand the following mastication loads applied simultaneously on all teeth (according to the considered options): the minimum level of 192 N when loading only incisors (No.1) and the maximum value of 1000 N when loading both premolars and molars (No.3). This conclusion was valid for both initial and deformed virtual supports.

For the studied RCD, the use of both perforated and solid PEEK frameworks enhanced its mechanical properties by 20–40% under different loading conditions, including the case with the deformed virtual support. Comparison of the perforated and solid PEEK frameworks showed that the presence of holes of the given diameter and locations reduced the mechanical properties of the base by ≤5% in some cases.

Calculation of SSSs of the RCD of the maxilla at low adhesion between the PEEK framework and the base

Since ideal adhesion between the base and the PEEK framework is difficult to ensure under real operational conditions, a case of its low level was considered in order to assess the played role. For this purpose, the contact properties were changed in the model of the RCD, namely, the contact stiffness and the separation stress were reduced down to 1 MPa that was an order of magnitude less than the contact stresses with ideal adhesion. So, the detachment of the PEEK framework from the base dome began immediately from the first steps of loading. Tab. 1 presents the load-bearing capacities of the base with the initial virtual support under several loading conditions. They were lower compared to those for ideal adhesion between the PEEK framework and the base (more negligible than those without a framework in some cases). This result was consistent with the practice of using reinforcing metal meshes [40]. Thereby, the use of PEEK for additive manufacturing of perforated frameworks could solve this issue.

Models	Option, No.			
	1	2	7	8
Without a framework, N	34	73	146	107
PEEK framework in the center (without adhesion), N	43	81	148	92
PEEK framework in the center (ideal adhesion), N	47	86	178	128

Table 1: The load-bearing capacities of the base with the initial virtual support under several loading conditions.

Fig. 13 shows distributions of the maximum principal stresses in the base, the PEEK framework for the RCD with the initial virtual support under the low adhesion (option No. 2, i.e. loading on four incisors at the angle of 0 °). In contrast to the above results for ideal adhesion, stresses concentrated in the base at the area of sockets caused by the development of displacements. Upon loading, the PEEK framework practically did not prevent bending of the base, which withstood the

same load as in its absence (and even lower in some cases). Thus, improving adhesion was a prerequisite for inserting the PEEK framework into the RCD.

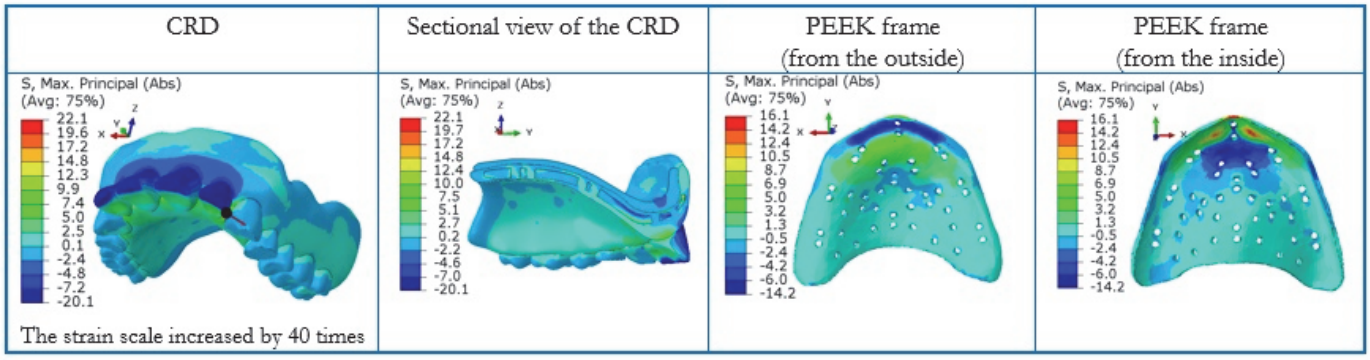

Figure 13: The distributions of the maximum principal stresses (MPa) in the base and the PEEK frameworkfor the RCD with the initial virtual support without adhesion (option No. 2).

Before concluding, the authors considered it necessary to note the following. The results obtained in this study were theoretical in nature, despite the fact that their formulation was based on the consideration of real objects and methods of their loading. For this reason, the reported data should not be regarded as an exact quantitative assessment, but rather as a recommendation for designing RCDs with reinforcing perforated PEEK frameworks.

The authors suggest three directions for the development of these investigations. Firstly, adhesion between the PEEK framework and the base dome can be improved by increasing the contact area, for example, by treating with supercritical carbon dioxide or mechanical texturing. Secondly, it is advisable to supplement the PEEK framework with stiffening ribs, for example, two ones on both sides along the entire dental arch, i.e. in areas of the greatest bending of the base. The ribs can increase its bending stiffness and prevent the movements in the contact between the base and the PEEK framework, as with low adhesion. Thirdly, failure of RCDs often occurs due to the cyclic pattern of applied loads, so it is important to carry out calculations on the fatigue life of the dental structures under such conditions.

Conclusions

The new approach was proposed and computer simulation of the deformation behavior of the RCD was performed for improving its mechanical properties. In this way, the perforated PEEK framework was installed in the dome of the PMMA base. For this dental structure, the model was developed taking into account the conditions of the attachment of the base, close to real ones. Namely, the prosthetic bed was simulated as the virtual support, for which the presence of 'accomodation zones' with different compliance of the oral mucosa was considered. The application of these boundary conditions represents the novelty when simulating deformation behavior and calculating the strength properties of the removable denture structures.

The calculations taking into account the deformed virtual support with ideal adhesion with the base showed that the mechanical properties decreased by ≤50% under some loading conditions, in contrast to the model with the initial virtual support.

Under different loading conditions, two cases of bending of the base were observed, which led to its failure. The first one was caused by the action of the turning moments (predominant under loading on the anterior teeth), while the second bending type (overbending) initiated in the area of its attachment to the alveolar ridge (predominant under loading on the lateral teeth). In the last case, both tensile and compressive stresses were localized in the existing notches for the frenulum and cords along the edge of the base under all applied loading conditions. Accordingly, they could be the regions of its failure, including due to the accumulation of fatigue damage.

The presence of the perforated PEEK framework in the PMMA base increased the load-bearing capacity of the RCD of the maxilla by 20–40% under different loading conditions (even taking into account alveolar bone resorption). This phenomenon was ensured by the more uniform distributions of stresses in the base and the reduction of its bending due to improved rigidity. Perforation decreased bending of the base to the greatest extent for the RCD with the deformed virtual support.

The greatest load-bearing capacity of the base was ensured by the location of the perforated PEEK framework on its inner side and in the center of the dome. At the same time, changing the location varied the load-bearing capacity of the RCD by ≤5%. The perforated framework located inside the PMMA base increased its stiffness. However, the presence of accommodation zones on the mucosa surface ensured the more comfortable wearing of the prosthesis. The presence of perforation in the PEEK framework reduced the load-bearing capacity of the base within 5% or did not change it (depending on the location of the PEEK framework).

Adhesion between the base and the PEEK framework played a decisive role. Its absence reduced the load-bearing capacity of the base to the level of the RCD without a framework.

Based on the obtained results, it was convincingly proven that the embedding of perforated reinforcing PEEK frameworks is a promising way to improve the load-bearing capacities of RCDs, considering the identified features of their behavior under typical operational loads. In doing so, further studies will focus on increasing the stiffness of the base due to modification of the framework design, as well as improving mechanical adhesion between the framework and the base through the variable perforation and other structural features.

ACKNOWLEDGEMENT

Sergey Panin, Svetlana Bochkareva and Iliya Panov acknowledge support from the project FWRW-2021-0010 through the government research assignment for ISPMS SB RAS.

ABBREVIATION

CAE - computer aided engineering,
FEM - finite element method,
PEEK - polyetheretherketone,
PMMA - polymethylmethacrylate,
RCD - removable complete denture,
SSS - stress–strain state,
XFEM - extended finite element method

REFERENCES

[1] Arutyunov, S.D. ed., (2021). Quality of life of patients with complete tooth loss and psychometric properties of the OHIP-20 DG questionnaire. Part 2. Monitoring at the stages of dental orthopedic treatment, Russian Dental J., 25(5), pp. 399–408. DOI: 10.17816/1728-2802-2021-25-5-399-408. (in Russian)

[2] Dye, BA. (2017). The Global Burden of Oral Disease: Research and Public Health Significance, J Dent Res., 96(4), pp. 361-363. DOI: 10.1177/0022034517693567.

[3] Ito, K. ed., (2015). JAGES Group. Individual- and community-level social gradients of edentulousness, BMC Oral Health., 15(34), DOI: 10.1186/s12903-015-0020-z.

[4] Rajaraman, V. ed., (2018). Ashish Effect of edentulism on general health and quality of life, Drug Invention Today, 10(4), pp. 549-553.

[5] Razak, P.A., ed., (2014). Geriatric oral health: a review article, J. Int. Oral Health, 6(6), pp. 110-116. PMID: 25628498; PMCID: PMC4295446.

[6] Porfiriev, B.N. ed., (2023). Development of Subsidized Prosthodontic Care: Socio-Economic Problems and Opportunities, Studies on Russian Economic Development, 34(1), pp. 68–76. DOI: 10.1134/S1075700723010161

[7] Bayraktar, G., Duran, O. and Guvener, B. (2003). Effect of glass fibre reinforcement on residual methyl methacrylate content of denture base polymers, J. Dent, 31(4), pp. 297-302. DOI: 10.1016/s0300-5712(03)00026-5. PMID: 12735925.

[8] Torres, A. ed., (2019). Technical quality of complete dentures: Influence on masticatory efficiency and quality of life, J. Prosthodont. 28, pp. 21-26.

[9] Kumari, R. and Bala, S. (2021). Assessment of Cases of Complete Denture Fracture, J. Pharm. Bioallied Sci., 13(2), pp. 1558-1560. DOI: 10.4103/jpbs.jpbs_284_21.

[10] Shinde, J. ed., (2022). Satisfaction in conventional acrylic complete denture patient with and without denture liners – a systematic review, Pan. Afr. Med. J., 42(296). DOI: 10.11604/pamj.2022.42.296.33035.
[11] Zafar, M.S. (2020). Prosthodontic Applications of Polymethyl Methacrylate (PMMA): An Update, Polymers (Basel), 12(10). DOI:10.3390/polym12102299
[12] Arutyunov, S.D. ed., (2002). Microbiological substantiation of the choice of base plastic for removable dentures, Stomatology, 3, pp. 4-8. (in Russian)
[13] Goodacre, B.J. and Goodacre, C.J. (2022). Additive Manufacturing for Complete Denture Fabrication: A Narrative Review, J. Prosthodont., 31(S1), pp. 47-51. DOI: 10.1111/jopr.13426. PMID: 35313025.
[14] Grachev, D.I. ed., (2023). Ranking Technologies of Additive Manufacturing of Removable Complete Dentures (RCD) by the Results of Their Mechanical Testing, Dentistry, 11(11). DOI: 10.3390/dj11110265
[15] Zeidan, A.A.E. ed., (2023). Evaluation of the Effect of Different Construction Techniques of CAD-CAM Milled, 3D-Printed, and Polyamide Denture Base Resins on Flexural Strength: An In Vitro Comparative Study, J. Prosthodont., 32(1), pp. 77-82. DOI: 10.1111/jopr.13514.
[16] Dhiman, R. and Chowdhury, S.R. (2009). Midline fractures in single maxillary complete acrylic vs flexible dentures, Med. J. Armed Forces India, 65, pp. 141–145.
[17] Tuominen, R. (2003). Clinical quality of removable dentures provided by dentists, denturists and laboratory technicians, J. Oral Rehabil., 30(4), pp. 347-52. DOI: 10.1046/j.1365-2842.2003.01055.x. PMID: 12631157.
[18] John, J., Gangadhar, S.A. and Shah, I. (2001). Flexural strength of heat-polymerized polymethyl methacrylate denture resin reinforced with glass, aramid, or nylon fibers, J. Prosthet Dent., 86(4), pp. 424-427. DOI: 10.1067/mpr.2001.118564. PMID: 11677538.
[19] Ladha, K. and Shah, D. (2011). An in-vitro evaluation of the flexural strength of heat-polymerized poly (methyl methacrylate) denture resin reinforced with fibers, J. Indian Prosthodont Soc., 11(4), pp. 215-220. DOI: 10.1007/s13191-011-0086-5.
[20] Murthy, H.B. ed., (2015). Effect of Reinforcement Using Stainless Steel Mesh, Glass Fibers, and Polyethylene on the Impact Strength of Heat Cure Denture Base Resin – An In Vitro Study, J. Int. Oral Health., 7(6), pp. 71-79.
[21] Singh, K. ed., (2016). Comparative evaluation of flexural strength of heat polymerised denture base resins after reinforcement with glass fibers and nylon fibres: An in vitro study, Adv. Hum. Biol., 6, pp. 91–4.
[22] Somani, MV. Ed., (2019). The effect of incorporating various reinforcement materials on flexural strength and impact strength of polymethylmethacrylate: A meta-analysis, J. Indian Prosthodont. Soc., 19(2), pp. 101-112. DOI: 10.4103/jips.jips_313_18.
[23] Istabrak, D. ed., (2022). Comparison of two resilient attachment systems for implant-/mucosa-supported overdentures with a PEKK framework: a clinical pilot study, Clinical Oral Investigations, 26, pp. 3707–3719. DOI: 10.1007/s00784-021-04342-4
[24] Karaseva, V.V. (2014). Prevention of frequent fractures of plate dentures by using a quartz mesh, Problems of Dentistry, 5, pp. 41–44. (in Russian)
[25] Karaseva, V.V. (2015). Use of reinforcing quartz mesh for prevention of fractures of bases of plate removable dentures in patients with through defects of the hard palate, Problems of Dentistry, 11(3–4), pp. 47–53. DOI: 10.18481/2077-7566-2015-11-47-53 (in Russian)
[26] van Meegen, H.G. and Kalk, W. (2011). Verbetering van een gebitsprothese door middel van relining of rebasing [Improvement of a removable complete denture by relining or rebasing], Ned Tijdschr Tandheelkd, 118(11), pp. 545-551. DOI: 10.5177/ntvt.2011.11.11167. PMID: 22235517.
[27] Hsu, Y.T. (2015). Consequences of relining on a maxillary complete denture: A clinical report, J. Prosthet. Dent., 114(1), pp. 13-6. DOI: 10.1016/j.prosdent.2014.11.012.
[28] Grachev, D.I. ed., (2023). Dental Material Selection for the Additive Manufacturing of Removable Complete Dentures (RCD), Int. J. of Molecular Sci., 24(7). DOI: 10.3390/ijms24076432
[29] Grachev, D.I. ed., (2022). Algorithm for designing a removable complete denture (RCD) based on the FEM analysis of its service life, Materials, 15(20). DOI: 10.3390/ma15207246.
[30] Chizhmakov, E.A. ed., (2024). Application of Polyethylene Terephthalate as a Denture Base Material for Manufacturing Temporary Removable Complete Dentures, Mech. Compos. Mater., 60, pp. 227–242. DOI: 10.1007/s11029-024-10186-2
[31] Jagger, D.C., Harrison A. and Jandt K.D. (1999). The reinforcement of dentures, J. Oral Rehabil., 26(3), pp. 185-194. DOI: 10.1046/j.1365-2842.1999.00375.x. PMID: 10194725.
[32] Aldegheishem, A. ed., (2021). Influence of Reinforcing Agents on the Mechanical Properties of Denture Base Resin: A Systematic Review, Polymers, 13(18), p.3083. DOI: 10.3390/polym13183083

[33] Removable plate denture with reinforced base: Pat. 2791989 RF / Arutyunov S.D., Dibirov T.M., Nersesov G.S., Stepanov A.G., Bagdasaryan G.G., Ordyan G.A., Grachev D.I. ; application 02/03/2022; publ. 03/15/2023, Bulletin. No. 8. – 13 p. (in Russian)
[34] Shcherbakov, A.S. ed., (1998). Orthopedic Dentistry, St. Petersburg, Foliot, 565 p. (in Russian)
[35] Kulazhenko, V.I. (1972). Using the amplitude of compliance of soft tissues of the prosthetic field to improve the quality of removable dentures, Stomatology, 1, pp. 34–36. (in Russian)
[36] Muslov, S.A. ed., (2023). Bioengineering aspects of oral mucosa: review and authors' research, Modern Issues of Biomedicine, 7(4). DOI: 10.24412/2588-0500-2023_07_04_37.
[37] PMMA. Matbase: the free and independent online materials properties resource. – URL: http://www.matbase.com/material-categories/natural-and-syntheticpolymers/commodity-polymers/material-properties-of-polymethyl-methacrylate-extruded-acrylicpmma.html#properties.
[38] Danilevsky, N. F. (1993). Periodontal diseases. Atlas, Medicine, Moscow.
[39] PEEK. Matbase: the free and independent online materials properties resource. – URL: https://web.archive.org/web/20071209134131/http://www.matbase.com/material/polymers/engineering/peek/properties.
[40] Vojdani, M. and Khaledi, A. A. R. (2006). Transverse Strength of Reinforced Denture Base Resin with Metal Wire and E-Glass Fibers, J. Dent., 3(4), pp. 167-172.